Monatshefte für Chemie 134, 679–692 (2003)
DOI 10.1007/s00706-002-0586-4

Monatshefte für Chemie
Chemical Monthly
Printed in Austria

Invited Review

Solubility Behavior in Ternary Water-Salt Systems under Sub- and Supercritical Conditions

Vladimir Valyashko* and **Marina Urusova**

Kurnakov Institute of General and Inorganic Chemistry, Russian Academy of Sciences, 119991 Moscow, Russia

Received September 25, 2002; accepted (revised) November 28, 2002
Published online April 24, 2003

Summary. Two main types of binary systems with distinctive solubility behavior under sub- and supercritical conditions were used to subdivide ternary water-salt systems into three classes. Characteristic features of solubility behavior and phase equilibria in ternary water-salt systems of each class at temperatures above 200°C are discussed on the basis of available experimental data and some conclusions obtained as a result of theoretical derivation of fluid and complete phase diagrams.

Keywords. Solubility; Phase diagram; Sub- and supercritical conditions; Water-salt systems; Critical and immiscibility phenomena.

Introduction

The solubility behavior of water-salt systems under sub- and supercritical conditions differs considerably from the low-temperature one. Not only the values of salt solubility, but also the types of solid–fluid equilibria are changed. At temperatures up to 100–200°C and at varying pressures, the diversity of solubility equilibria is mainly due to the abundance of crystalline hydrates. At higher temperatures the crystalline hydrates no longer exist, but equilibria of solid phase with immiscible liquids, critical or supercritical fluids (absent at lower temperatures), becomes common.

In contrast with the majority of gas-water, organic, and organic-water systems, where supercritical equilibria do not typically include a solid phase, water-salt equilibria at sub- and supercritical conditions of water usually contain a solid phase

* Corresponding author. E-mail: Valyashko@IGIC.RAS.RU
Dedicated to Prof. Dr. *H. Gamsjaeger* on the occasion of his 70th birthday anniversary

because the most salt components (which are any inorganic compounds) have melting temperatures higher than the critical temperature of water. However, if such a relationship between melting and critical temperatures of nonvolatile and volatile components takes place, any system should have the same supercritical solid–fluid equilibria.

The main objective of this paper is to survey the general features of solubility behavior in ternary sub- and supercritical water-salt mixtures using both the available experimental data and theoretical concepts. Phase equilibria of ternary systems depend in a large part on phase behavior in binary subsystems. Therefore, the presentation of the material starts from a description of the main types of binary phase diagrams and solubility behavior in binary mixtures.

Binary Systems

There are two types of solubility behavior in binary systems with components of different volatility and solid-supercritical phase equilibria [1–5]. Binary systems of type **1** (such as NaCl–H_2O, KCl–H_2O, K_2CO_3–H_2O, NaOH–H_2O, CO_2–CH_4, *etc*.) are characterized by increasing salt (nonvolatile component) solubility in the liquid phase with temperature (positive temperature coefficient of solubility (t.c.s.)) at vapor and higher pressures up to the melting point of the salt, and by the absence of critical phenomena between liquid and gas (vapor) in solid saturated solutions (Fig. 1). The vapor pressure of the three-phase (L–G–S) solubility curve has a maximum (Fig. 2) where the pressure can be as high as 40 MPa in some water-salt systems, but never reaches the critical (L=G) pressure at the same temperature. The available experimental data in a temperature range up to 500–600°C show that the critical curves L=G of water-salt systems originating in the critical point of water are located at pressures in the vicinity of the critical isochore of water [6]. If the pressure becomes lower than the vapor pressure of the solid saturated solution in three-phase equilibrium (L–G–S), the liquid phase disappeares and the solubility of

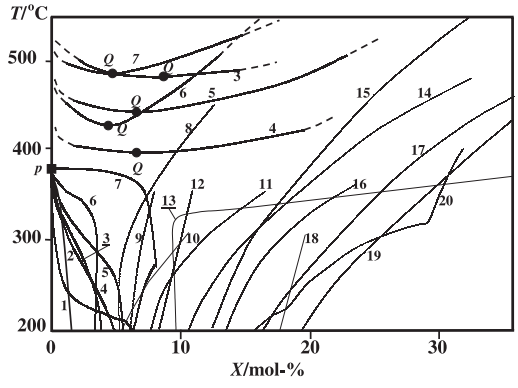

Fig. 1. Composition of the liquid solutions in three-phase solubility equilibria L–G–S and L_1–L_2–S (solubility curves) for the binary water-salt systems of type **2** (heavy lines 1–7) and type **1** (thin lines 8–20); 1–Na_3PO_4, 2–NaF, 3–Na_2CO_3, 4–Li_2SO_4, 5–Na_2SO_4, 6–K_2SO_4, 7–$BaCl_2$, 8–Na_2WO_4, 9–Na_2SeO_4, 10–KIO_3, 11–Na_2MoO_4, 12–K_2CrO_4, 13–LiOH, 14–$Sr(NO_3)_2$, 15–NaCl, 16–Na_2CrO_4, 17–KCl, 18–Cs_2SO_4, 19–NaBr, 20–$SrCl_2$

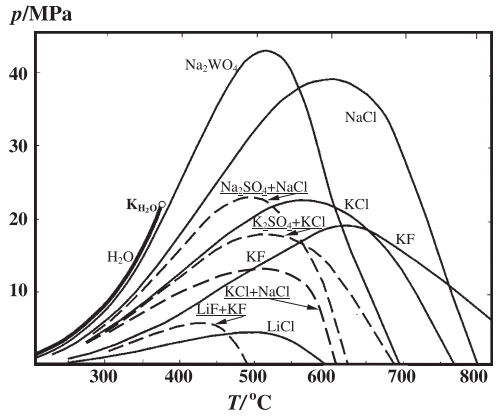

Fig. 2. *p-T* Projections of the three-phase solubility curves (L–G–S) in binary systems of type **1** (solid lines), eutonic curves (L–G–S_1–S_2) in ternary systems (dashed lines), and liquid–gas curve for pure H_2O (heavy line)

the same salt in the low-density vapor (gas) phase becomes negligible excluding the narrow temperature range just near the melting point of the salt. The type **1** solubility behavior is observed in systems where the melting point of the salt (nonvolatile) component can be both lower and higher than the critical point of water (volatile component).

In the case of the type **2** systems (such as Na_2CO_3–H_2O, Na_2SO_4–H_2O, Na_3PO_4–H_2O, SiO_2–H_2O, naphthalene–ethylene, *etc*.) the melting temperature of the salt (nonvolatile) component must necessarily be higher than the critical temperature of water (volatile component) and the salt solubility in liquid solution decreases with temperature (negative t.c.s.) under subcritical conditions (Fig. 1). As a result the compositions of saturated liquid and vapor solutions approach each other and become identical in the first critical endpoint ''p'' (L=G–S), where the critical phenomenon between liquid (L) and gas (vapor; G) takes place in equilibrium with the solid phase (S) at temperatures just above the critical temperature of pure water [6]. Critical phenomena between liquid and gas give rise to supercritical fluid equilibria where a homogeneous supercritical fluid phase is not separated into liquid and gas at any pressure. The observed solubility of type **2** salts in supercritical fluids is kept very low up to high pressures, which are much above the pressures of liquid phase appearance in the systems of type **1** at the same temperatures. A separation of homogeneous supercritical fluid into two solutions takes place only with increasing temperature until the high temperature branch of the three-phase solubility curve originating in the melting point of the pure salt (nonvolatile component) and terminates at the second critical endpoint ''Q'' (critical phenomena in solid saturated solutions). Thus, the supercritical fluid region occurs in the temperature range between the critical endpoints p and Q (Fig. 1). Critical endpoints p end the critical curves L=G originating in the critical point of water (K_{H_2O}) and lie close together (the maximum deviation of p from K_{H_2O} (near 10°C) is observed in the system H_2O–$BaCl_2$ [7]). The conditions of critical endpoints Q in water-salt systems are much wider and depend on the nature of salt (nonvolatile) component. The examples of the type **2** systems in Fig. 1 show a small difference between the

temperatures of points p and Q (less than 100°C). However, the critical pressures of points Q are rather high (from 67 to 160 MPa) because these systems are complicated by immiscibility phenomena and the critical phenomena at points Q belong to the immiscibility equilibria L_1=L_2–S, whereas the critical endpoint p has the equilibrium L=G–S.

The available experimental data on phase equilibria and the generation of phase diagrams from the equations of state show four main types (types **a**–**d**) of fluid phase behavior [5, 6, 8–10], which can be found in the binary systems of both types (types **1** and **2**) of solubility behavior. Type **a** of fluid phase behavior is characterized by the absence of immiscibility phenomena, and only one heterogeneous equilibrium L–G and one critical equilibrium L=G are present. Types **b**, **c**, and **d** are distinguished by several fluid phase heterogeneous and critical equilibria due to the presence of various immiscibility regions. Phase diagrams of type **b** have a so-called ''limited'' or ''closed-loop'' immiscibility region bounded by three-phase monovariant curve L_1–L_2–G and critical curve L_1=L_2 that does not intersect with the second critical curve L=G. In the case of type **d** phase diagrams, the critical curves L=G and L_1=L_2 are intersected and the critical curve (L=G) starting in the critical point of water is interrupted by a 3-phase immiscibility region L_1–L_2–G at the upper critical endpoint R (L_1=G–L_2). The second branch of the critical curve begins at the critical point (L=G) of the salt component, passes continuously from L=G into the L_1=L_2 critical curve and ends at the lower critical endpoint N (L_1=L_2–G) of the immiscibility region. Type **c** of fluid phase behavior is characterized by the presence of two separated immiscibility regions of type **b** and **d**.

The nomenclature of various types of binary complete phase diagrams or phase behavior in the binary systems contains a number (**1** or **2**) reflecting the features of solid–fluid equilibria and a letter (**a**, **b**, **c**, or **d**) corresponding to the type of fluid phase behavior. More detail information about the nomenclature and systematic classifications of binary fluid and complete phase diagrams can be found in Refs. [5, 10].

Stable three-phase immiscibility regions L_1–L_2–G of various types occur in the systems of type **1**, whereas in the systems of type **2** this three-phase equilibrium is usually metastable. Therefore an attribution of supercritical fluid phase behavior in the type **2** systems is a complicated problem. However, if the heterogeneous fluid equilibria occur at pressures well above the pressure of a critical isochore of water, the equilibrium fluids most probably belong to liquid–liquid immiscibility but not to liquid–gas equilibria. There are also another criteria to detect the existence of an immiscibility region in the binary systems of type **2** [5, 11].

It is important to note that all binary water-salt systems of type **2** studied in details at high temperatures and pressures, such as aqueous systems with $BaCl_2$, Li_2SO_4, K_2SO_4, $KLiSO_4$, Na_2CO_3, Na_2SiO_3, $Na_2Si_2O_5$, Na_2SO_4, and SiO_2 are complicated by a metastable three-phase immiscibility region of type **d** and have the second critical endpoint Q at the equilibrium L_1=L_2–S.

Ternary Systems

The major features of phase behavior in ternary systems are determined by the types of phase diagrams of constituting binary subsystems, since all binary equilibria

spread into the three-component region of composition and take part in the generation of ternary phase diagrams. Different versions of ternary phase diagrams of the same types of binary subsystems can appear mainly due to the various intersections of the spreading elements of binary diagrams. Therefore the types of constituent binary subsystems can be used for preliminary systematization of ternary phase behavior and for designation of the various classes of ternary systems. The binary anhydrous salt systems universally belong to type **1**. A division of binary water-salt subsystems into types **1** and **2** gives the following classification of ternary systems: (i) ternary systems with two binary water-salt subsystems of type **1** (ternary class **1-1-1**); (ii) ternary systems with binary water-salt subsystems of types **1** and **2** (ternary class **1-2-1**); (iii) ternary systems with two binary water-salt subsystems of type **2** (ternary class **2-2-1**).

The general features of solubility, immiscibility, and critical behavior in ternary systems of three major classes will be formulated as a result of reviewing the available experimental data on hydrothermal equilibria and some theoretical conclusions obtained in a process of ternary phase diagram derivation by the method of continuous topological transformation [5, 10, 12].

Ternary Systems with Binary Water-Salt Subsystems of Type **1**

The simplest ternary phase behavior is observed in ternary water-salt systems where the both binary water-salt and anhydrous subsystems belong to type **1** without immiscibility phenomena (binary type **1a**). Systems H_2O–NaCl–KCl [13–16], H_2O–KCl–KBr [17], H_2O–KCNS–KCl (KBr, KI) [18], H_2O–NH_4NO_3–$Pb(NO_3)_2$ [19], H_2O–NaCl–NaOH [20], H_2O–LiOH–NaOH, H_2O–LiOH–KOH, H_2O–LiOH–RbOH [21] belong to this ternary class and were studied more in detail at elevated temperatures and pressures.

The general feature of these systems and other ternary water-salt systems with eutectic phase relations in binary subsystems is the appearance of eutonic equilibria, where two solid phases of components coexist with liquid and vapor solutions. Each two three-phase solubility surfaces (L–G–S) are intersected along with the monovariant eutonic curves (L–G–S_1–S_2). These curves are characterized by local extreme parameters and join the eutectic point of ternary system (L–G–S_A–S_B–S_C) with the eutectic points of binary subsystems (L–G–S_A–S_B; L–G–S_A–S_C; L–G–S_B–S_C). Figure 3 shows the projection of three-phase solubility surfaces in the system NaCl–KCl–H_2O on the triangle of composition as a set of isothermal cross-sections with concentration maxima on the polythermal eutonic curve. The eutonic curve passes through a maximum of vapor pressure, which is much lower than the similar maximum on the three-phase solubility curves in binary water-salt subsystems (see Fig. 2).

The occurrence of an immiscibility region makes the phase diagrams more complex but does not change the eutonic behavior of solubility surface in a ternary system. If only one binary subsystem has an immiscibility region (types **1b**, **1c**, and **1d**), it should disappear in ternary solutions. The immiscibility regions while spread from two binary subsystems can either merge in the three-component range of composition or disappear in ternary solutions and be separated by a miscibility region.

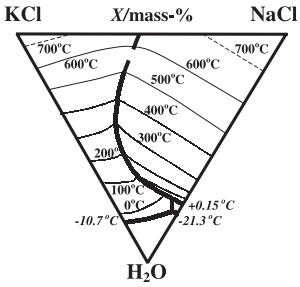

Fig. 3. Solubility isotherms at vapor pressures in the system KCl–NaCl–H_2O [15]; heavy lines give the composition of eutonic solutions saturated with two solid phases

The disappearance of the type **d** immiscibility region was studied in the system H_2O–NaCl–$Na_2B_4O_7$ [22], where only the binary subsystem H_2O–$Na_2B_4O_7$ is complicated by a immiscibility region. This immiscibility region of type **1d** spreading from the binary subsystem H_2O–$Na_2B_4O_7$ is terminated by the tricritical point (TCP) RN (L_1=L_2=G), where three coexisting fluid phases become simultaneously identical. The TCP is a point of intersection of two monovariant critical curves L_1=L_2–G and L_1=G–L_2 (Fig. 4a) (which were located using the experimental data on vapor pressure for the ternary solutions in the vicinity of these critical curves) at 408±2°C, 295±5 kg/cm^2, 2.2±0.2 mol-% NaCl, 2.2±0.2 mol-% $Na_2B_4O_7$.

The tricritical point RN was also found in the HgI_2–PbI_2–H_2O system, which has two different types of immiscibility regions in the subsystems HgI_2–H_2O (type **1b′**) and PbI_2–H_2O (type **1d′**) [23]. Figure 4 is a *T*-X^* projection of a ternary phase diagram with monovariant curves plotted using the experimental data obtained by

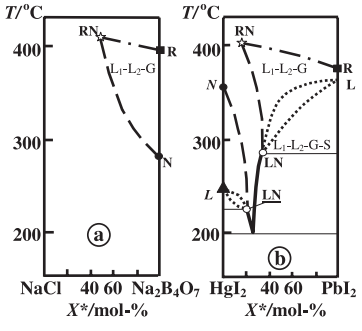

Fig. 4. *T*-X^* projections of immiscibility regions in ternary systems NaCl–$Na_2B_4O_7$–H_2O [22] (a) and HgI_2–PbI_2–H_2O [23] (b).

Solid square and circle are the critical endpoints L_1=G–L_2 (R) and L_1=L_2–G (N) in binary subsystems, solid triangles denote the nonvariant equilibrium L_1=L_2–G–S (L) in binary systems, open star and circle are the tricritical point L_1=L_2=G (RN) and invariant critical point L_1=L_2–G–S (LN) in the ternary system; dashed lines are the monovariant critical curves L_1=L_2–G; dot-dashed lines are the monovariant critical curves L_1=G–L_2; dotted lines show the composition of coexisting solutions (tentative data) in the equilibrium L_1–L_2–G–S; solid lines show the composition of liquid phase saturated with vapor and solid phase (L–G–S); $X^*=100X_1/(X_1+X_2)$, where X_1 and X_2 are the molar amounts of salts in aqueous solution

the method of visual observation of the phase transformations in sealed thick-walled glass tubes. The immiscibility region of type **d**, spreading from the binary subsystem PbI_2–H_2O, is bounded by two monovariant critical curves L_1=L_2–G and L_1=G–L_2 and ends in the tricritical point RN (at 401±2°C and 65±2 mass-% HgI_2, 10±2 mass-% PbI_2), where both critical curves intersect. Another immiscibility region of type **b** spreading from the subsystem HgI_2–H_2O is terminated by the invariant critical point in saturated solutions NL (L_1=L_2–G–S), where the critical curve L_1=L_2–G is intersected with the four-phase monovariant curve L_1–L_2–G–S. The immiscibility region of type **b** can be terminated also by the double critical endpoint N′N (L_1=L_2–G) in ternary systems when two critical endpoints of the same nature L_1=L_2–G coincide. The most probable behavior occurs in systems where the immiscibility region of type **b** does not intersect with the solubility surface, however, such ternary water-salt systems have not been studied up to now.

Both binary subsystems HgI_2–H_2O and PbI_2–H_2O are characterized by a nonvariant equilibrium L (L_1–L_2–G–S) in contrast with the system $Na_2B_4O_7$–H_2O where the immiscibility region is not interfered by the occurrence of a solid phase. As a result the low-temperature parts of both immiscibility regions are hidden by the solid phases of HgI_2 and PbI_2, and the solubility curves in binary subsystems of types **1b′** and **1d′** are interrupted by a nonvariant point L (L_1–L_2–G–S) and have a jump in the composition of the saturated liquid solution.

Figure 4 shows the eutonic behavior of solubility surfaces of HgI_2 and PbI_2, where both surfaces have a slope directed onto the eutonic composition at the temperature minimum. However, both solubility surfaces become complicated by the immiscibility in the saturated solutions (L_1–L_2–G–S) that ends in nonvariant critical points LN (L_1=L_2–G–S). Theoretical derivation of ternary phase diagrams shows that the immiscibility of liquids may occur in the eutonic solutions (L_1–L_2–G–S_1–S_2) as a result of merging together both immiscibility regions (L_1–L_2–G–S) while spread from the two binary subsystems. Such phase behavior was not encountered experimentally but several versions of intersection of three-phase immiscibility regions (L_1–L_2–G) spreading from two binary subsystems were studied in ternary carbon dioxide–*n*-alkane–1-alkanol systems [24].

Ternary Systems with Binary Water-Salt Subsystems of Types **1** *and* **2**

The general feature of ternary systems with binary water-salt systems of different types (types **1** and **2**) is the change of the temperature coefficient of solubility (t.c.s.) sign from negative to positive in ternary solutions. As a result the three-phase solubility surface (L–G–S) attains a new configuration near the binary subsystem of type **2**. The new configuration of the solubility surface is shown in Fig. 5 as an intersection of solubility isotherms. Eutonic solutions, as well as in the ternary systems with two binary water-salt subsystems of type **1** are characterized by positive t.c.s. and a pressure maximum on the eutonic curves (see the eutonic curves for the systems NaCl–Na_2SO_4–H_2O [25], KCl–K_2SO_4–H_2O [26], and LiF–KF–H_2O [27] in Figs. 2, 5).

The negative t.c.s., which is typical of dilute hydrothermal solutions saturated with a salt of type **2**, becomes positive when the total solution concentration increases up to 2–15 mol-% of the salt [5, 28] depending on the charge of the ions.

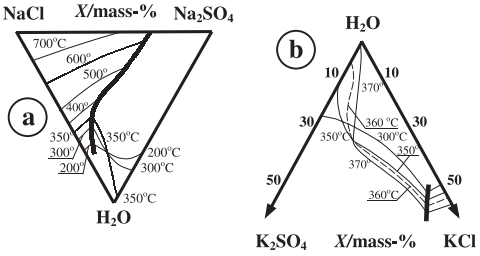

Fig. 5. Solubility isotherms at vapor pressure in the systems NaCl–Na_2SO_4–H_2O [25] (a) and KCl–K_2SO_4–H_2O [26] (b).

Solid and dashed lines show the composition of solid saturated liquid solutions at vapor pressure; heavy lines give the composition of liquid solutions saturated with two solid phases at vapor pressure (eutonic curves)

The sign of t.c.s. is changed at 13–15 mol-% in the system NaF–(NaCl + KCl)–H_2O (1:1 electrolytes), at 8–12 mol-% in ternary systems with 1:1 (NaCl, KCl, NaOH, KNO_3, $NaNO_3$) electrolytes of type **1** and 1:2 (Na_2SO_4, Na_2CO_3, K_2SO_4) or 2:1 ($Ca(OH)_2$) electrolytes of type **2**, and at <5.5 mol-% in the systems $CaCl_2$–$CaSO_4$–H_2O, $CaCl_2$–CaF_2–H_2O, where the main part of concentration is produced by 2:1 electrolyte of type **1** ($CaCl_2$) whereas the concentrations of the type **2** salts ($CaSO_4$, CaF_2) are very low [29]. Special analyses of available experimental data for various properties (electric conductivity, volume properties, and spectroscopic characteristics) of hydrothermal electrolyte solutions over a wide range of composition show the change of property behavior from ''water-like'' to ''melt-like'' in the same concentration region and permit to conclude that the system of hydrogen bonds in dilute solutions transforms into the system of ionic bonds in strong electrolyte solution at the concentrations of the transition region [28]. A drastic transformation of the aqueous solution structure from water-like to melt-like produces not only a change in the behavior of t.c.s and other solution properties. Liquid–liquid immiscibility in aqueous electrolyte solutions appears in the transition region of concentration where the occurrence of critical phase compositions was established for equilibria L_1=L_2, L_1=L_2–G (N), L_1=L_2–S (Q).

Another characteristic feature of ternary systems with binary water-salt subsystems of type **1** and **2** is a disappearance of supercritical fluid equilibria as the second salt component (the type **1** salt) is added to the binary subsystem of type **2**. A separation of homogeneous supercritical fluid (spreading from the binary subsystem of type **2**) into liquid–gas or liquid–liquid mixtures begins with the critical phenomena in solid saturated solutions. The border between the regions of homogeneous supercritical fluid and heterogeneous fluid equilibria is the ternary monovariant critical curve between the critical endpoints p and Q in binary subsystem of type **2**. If both endpoints have the same equilibrium L=G–S, the nature of the critical curve pQ is evident. Most of water-salt systems of type **2**, as it was mentioned above, are complicated by a metastable three-phase immiscibility region, and the critical endpoints p and Q have different nature (L=G–S and L_1=L_2–S). Hence, the metastable immiscibility region extends from the binary subsystem into the ternary one. However, a plausible transition of three-phase immiscibility region into the stable equilibria was not observed in most of the studied ternary water-salt

systems. This means that the disappearance of a three-phase immiscibility region takes place under metastable conditions. Nevertheless, the tie-line form of solubility isotherms (such as the 360 and 370°C isotherms in Fig. 5) clearly shows that the metastable immiscibility region takes place very close to the stable solubility surface. The transition of the metastable immiscibility region into stable equilibria through the immiscibility of solid saturated solutions at vapor pressure was established in the H_2O–Na_3PO_4–Na_2HPO_4 system [30, 31] where both water-salt subsystems have the type **d** three-phase immiscibility region that is stable in the H_2O–Na_2HPO_4 system and metastable in the H_2O–Na_3PO_4 system.

In the case when the three-phase immiscibility region spreading from the binary subsystem of type **2** disappears under metastable conditions a homogeneous supercritical fluid region is bounded by a monovariant critical curve pQ. This curve starts in the critical endpoint p as a critical endpoint locus of the nature L=G–S and transforms continuously into the equilibrium L_1=L_2–S with increasing of temperature and pressure on the way to the critical endpoint Q.

The first experimental data on a behavior of the critical curve pQ in a ternary system with metastable three-phase immiscibility region were obtained recently for the system H_2O–Na_2CO_3–K_2CO_3 shown in Figs. 6 and 7. Vapor pressure measurements of unsaturated ternary solutions at 425°C show that the vapor pressure is increasing upon addition of Na_2CO_3 to the aqueous K_2CO_3 solutions in spite of a general increase in concentration. As a result the pressure of critical curve L=G, which is originated in the critical point K (L=G) of the aqueous K_2CO_3 solution and bounded the isothermal two-phase region L–G spreading from the binary K_2CO_3–H_2O system, increases with increasing of the Na_2CO_3 content. The two-phase region L–G (shown by the shaded parts of isobaric cross-sections in Fig. 6) is limited by the critical curve L=G (K-pQ) from one side and by the three-phase region of solid saturated solutions L–G–$S_{Na_2CO_3}$ from the other side. The

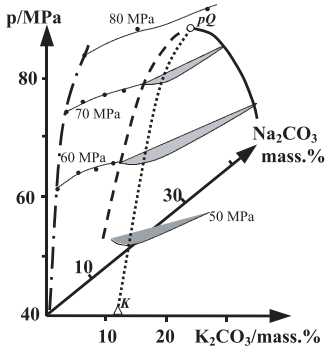

Fig. 6. Three-dimensional phase *p-X* diagram of the ternary system Na_2CO_3–K_2CO_3–H_2O at 425°C. Point K (solid triangle) is the critical point L=G in the binary system K_2CO_3–H_2O at 425°C; point pQ (open circle) is the critical point L=G–$S_{Na_2CO_3}$ (or L_1=L_2–$S_{Na_2CO_3}$) in the ternary system; the dot-dashed line is the solubility isotherm of the binary subsystem Na_2CO_3–H_2O in the supercritical fluid region; dashed and solid lines show the composition of vapor and one (or two) liquid solution(s) saturated with solid Na_2CO_3 in the ternary system; dotted line is the critical curve L=G (or L=G, L_1=L_2) between critical points K and pQ; thin lines show the isobaric cross-sections of two-phase region L–G (or L–G, L_1–L_2) (shaded parts) and the solid saturated fluid solution

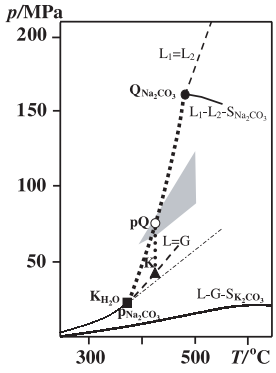

Fig. 7. *p-T* Projection of supercritical phase behavior in K_2CO_3–H_2O, Na_2CO_3–H_2O, and K_2CO_3–Na_2CO_3–H_2O systems [33, 34].

Solid square is the critical point L=G of water (K_{H_2O}) and the first critical endpoint $p_{Na_2CO_3}$ (L–G–S) in the system Na_2CO_3–H_2O; the solid circle is the second critical endpoint $Q_{Na_2CO_3}$ (L_1=L_2–S); open circle is the critical point pQ (L_1=L_2–S) of the ternary system at 425°C; the solid triangle is the critical point K (L=G) of the system K_2CO_3–H_2O. The thin line is the monovariant curve L–G of pure H_2O and the low temperature branch of three-phase solubility curve L–G–S in the system Na_2CO_3–H_2O; the thin dot-dashed line is the critical isochore of pure water; the solid lines are the three-phase monovariant curves L–G–S in the system K_2CO_3–H_2O and L_1–L_2–S in the system Na_2CO_3–H_2O; the dashed lines are the monovariant critical curves L=G in the system K_2CO_3–H_2O and L_1=L_2 in the system Na_2CO_3–H_2O; the dotted lines are the critical curves L=G–$S_{Na_2CO_3}$ (L_1=L_2–$S_{Na_2CO_3}$) and L=G (L_1=L_2) at 425°C in the ternary system; the shaded region is explained in the text

compositions of saturated solutions become identical in the critical point pQ, which belongs to the ternary critical curve pQ discussed above. The leftward lines of isobaric cross-sections at 60 and 70 MPa situated between the solubility isotherm of Na_2CO_3 in the subsystem Na_2CO_3–H_2O and the three-phase region L–G–$S_{Na_2CO_3}$, and the cross-section at 80 MPa show the surface of composition of homogeneous supercritical fluid saturated with solid Na_2CO_3, which is broken by the three-phase region at pressures below the critical point pQ (Fig. 6).

Figure 7 shows the pressure–temperature projections of non- and monovariant equilibria in the binary subsystems Na_2CO_3–H_2O and K_2CO_3–H_2O, and in the ternary system Na_2CO_3–K_2CO_3–H_2O that permit to discuss the nature of the critical curve pQ at 425°C, whether it is L=G–$S_{Na_2CO_3}$ or L_1=L_2–$S_{Na_2CO_3}$. Although we have no final resolution of this issue, there are two circumstantial evidences that the heterogeneous equilibria and critical phenomena at 425°C and 60–80 MPa are characterized by liquid–liquid immiscibility.

The first evidence is the occurrence of the mentioned temperature and pressure above the region around the critical isochore of water where the critical curves L=G of water-salt systems occur. The critical isochore of water and the critical curve L=G of the system K_2CO_3–H_2O in Fig. 7 show the *p-T* conditions where a continuous transition of supercritical aqueous fluids from gas-like to liquid-like state is started. The shaded region in Fig. 7 is a region where the experimental data on phase equilibria in the binary systems K_2SO_4–H_2O and $KLiSO_4$–H_2O show the existence of liquid–liquid equilibria. The second critical endpoints Q (L_1=L_2–S)

were found at 386°C and 60 MPa in the $KLiSO_4$–H_2O and at 430°C and 67 MPa in the K_2SO_4–H_2O systems [32, 33]. The borderlines of the shaded region were drawn between these points and parallel to the critical isochore and critical curve L=G. Thus, one can conclude that critical point pQ occurs on the border where the supercritical aqueous fluid can have liquid-like properties.

The second evidence is a good agreement in the compositions of the transition region of concentration obtained from the experimental data on the change of t.c.s. sign in the systems Na_2CO_3–H_2O and Na_2CO_3–K_2CO_3–H_2O. The sign of t.c.s. is changed in the concentration range 6.5–8 mol-% in the high-pressure equilibria L–$S_{Na_2CO_3}$ and L_1–L_2–$S_{Na_2CO_3}$ of the binary subsystem Na_2CO_3–H_2O. An intersection of the solubility isotherms (L–G–$S_{Na_2CO_3}$) at the vapor pressure in the system Na_2CO_3–K_2CO_3–H_2O is observed at general concentrations 5–7 mol-% of liquid solution. The concentration of the transition region for ternary solutions Na_2CO_3–K_2CO_3–H_2O obtained from the composition of the critical solution in equilibrium with solid Na_2CO_3 at 425°C (point pQ) is 5.5–6.5 mol-%. It should be noted that any point of the critical curve pQ is a starting point for two solid saturated solutions with the different signs of t.c.s. However, in the case of two liquid solutions the compositions of the critical phase lie inside the transition region of concentration, whereas the composition of the critical phase where the properties of liquid and vapor (gas) solutions become identical usually does not occur in the transition region. For instance, the available experimental data show that the composition of critical curves L=G in binary water-salt systems of type **1** occurs in a concentration range of 1–3.5 mol-% at 425°C.

Ternary Systems with Binary Water-Salt Subsystems of Type **2**

Two types of ternary phase behavior were established in the experimental studies of ternary systems with two binary water-salt subsystems of type **2**. For most aqueous systems with high melting point oxides and alumino-silicates, such as $NaAlSi_3O_8$–$KAlSi_3O_8$–H_2O, SiO_2–$NaAlSi_3O_8$–H_2O, SiO_2–$KAlSi_3O_8$–H_2O, SiO_2–$CaAl_2Si_2O_8$–H_2O, CaO–SiO_2–H_2O, *etc*. [35–37], the phase behavior of ternary mixtures is very similar to the binary ones. Supercritical fluid equilibria observed for ternary mixtures at any ratio of salt components, two branches of solubility (and eutonic) curves, and high pressures of the monovariant critical curves joining the second critical endpoints Q, show that a three-phase immiscibility region is retained under metastable conditions as well as in binary subsystems. In contrast to the eutonic curves in ternary systems of other classes, in these ternary systems the eutonic curves between the eutectic points of the ternary system and the binary anhydrous subsystem consist of two separated low- and high-temperature branches (as well as the solubility curves in binary systems of type **2**). However, the eutonic equilibria (L–G–S_1–S_2, L_1–L_2–S_1–S_2) in these ternary systems are also characterized by the highest concentrations and minimum vapor pressure in isothermal cross-sections and by extreme temperatures in isobaric sections.

Another type of phase behavior takes place when the metastable immiscibility region becomes stable in ternary solutions. As a result the joint solubility of the two salt components increases drastically, because the eutonic curve is separated from the solubility curves in the binary water-salt subsystems by the immiscibility

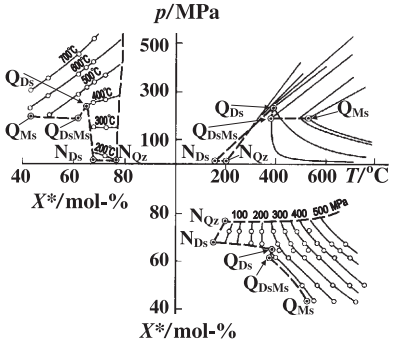

Fig. 8. p-X^*, p-T and T-X^* projections of the critical surface $L_1{=}L_2$ and monovariant curves of the system SiO_2–Na_2O–H_2O [38].

Dots in circles are the critical endpoints Q_{Ms} and Q_{Ds} ($L_1{=}L_2$–S) in binary Na_2SiO_3–H_2O and $Na_2Si_2O_5$–H_2O subsystems and the ternary critical endpoints N_{Qz} and N_{Ds} ($L_1{=}L_2$–G–S), and Q_{DsMs} ($L_1{=}L_2$–S_{Ds}–S_{Ms}); Qz is quartz (SiO_2); Ds is disilicate ($Na_2Si_2O_5$); Ms is metasilicate (Na_2SiO_3); open circles are the experimental points; dashed lines are the critical curves $L_1{=}L_2$–S and $L_1{=}L_2$–G; solid lines are the isothermal (p-X^* projection) or isobaric (T-X^* projection) cross-sections of the critical surface $L_1{=}L_2$; solid lines on the p-T projection are the cross-sections of the critical and solubility surfaces at constant SiO_2/Na_2O ratio in the mixtures; $X^*{=}100X_{SiO_2}/(X_{SiO_2}{+}X_{Na_2O})$, where X_{SiO_2} and X_{Na_2O} are the molar amounts of SiO_2 and Na_2O in aqueous solution

region. The t.c.s in eutonic solutions becomes positive and critical phenomena in these solutions saturated with two solid phases are absent.

Such behavior was found in the ternary systems H_2O–SiO_2–$Na_2Si_2O_5$ [38] and H_2O–K_2SO_4–$KLiSO_4$ [39]. As one can see from Fig. 8, the immiscibility region becomes stable when the $SiO_2{+}Na_2Si_2O_5$ mixture contains 65–80 mol-% SiO_2 as indicated by a decrease of temperature and pressure of the critical surface up to vapor pressures at 200°C.

Figure 8 also depicts another type of phase behavior in the ternary system $Na_2Si_2O_5$–Na_2SiO_3–H_2O, where the eutonic solution is terminated by the second critical endpoint Q_{MsDs} similar to the solubility curves in the binary subsystems H_2O–$Na_2Si_2O_5$ and H_2O–Na_2SiO_3 that are terminated in the critical endpoints Q_{Ms} and Q_{Ds}. This example demonstrates that one ternary class can have various types of phase behavior and several versions of phase diagram.

Conclusions

In this contribution we have tried to underline an intimate relationship between phase behavior in binary and ternary systems which permits to make some general conclusions. All available experimental data in ternary systems show that most ternary phase equilibria are equilibria spreading from the binary subsystems and the equilibria, which are a result of an intersection of these ''spreading'' equilibria between each other. Totally new equilibria appear only in the case when the ternary solid phase is generated as a product of chemical reaction between the three components. Consequently, the most probable versions of ternary phase behavior can be predicted if the phase diagrams of binary subsystems are known and the information about metastable equilibria in binary mixtures is available.

The last remark is very important because careful examination of experimental data and the results of thermodynamic calculations of phase diagrams show that the fluid equilibria do not disappear after intersection with a crystallization surface. Fluid equilibria suppressed by solidification of a component transform into metastable equilibria that can be turned into stable ones if the conditions are changed. For instance, if the number of components is increased or one component is exchanged by another.

Acknowledgments

This work was supported by the Russian Fondues of Basic Research under Grant No. 01-03-32770, U.S. Civilian Research and Development Foundation (Grant No. RC1-2210) and by the INTAS Project No. 00-640.

References

[1] Van der Waals JD, Kohnstamm Ph (1927) Lehrbuch Thermostatik. vol I, II. Verlag J Am Barth, Leipzig
[2] Ricci EJ (1951) The Phase Rule and Heterogeneous Equilibria. Van Nostrand, Toronto New York London
[3] Morey GW, Chen WT (1956) J Amer Chem Soc **78**: 4249
[4] Ravich MI (1974) Water-Salt Systems at Elevated Temperatures and Pressures Nauka, Moscow, p 150
[5] Valyashko VM (1990). Phase Equilibria and Properties of Hydrothermal Systems Nauka, Moscow
[6] Valyashko VM, Urusova MA (2001) Zh Fizich Khimii **75**: 1269
[7] Valyashko VM, Urusova MA, Kravchuk KG (1983) Dokl Akad Nauk SSSR **272**: 390
[8] Scott RL, Van Konynenburg PN (1970) Faraday Discuss Chem Soc **49**: 87
[9] Boshkov LZ (1987) Dokl Akad Nauk SSSR **294**: 901
[10] Valyashko VM (2002) Phys Chem Chem Phys **4**: 1178
[11] Valyashko VM (1995) Pure & Appl Chem **67**: 569
[12] Valyashko VM (2003) Pure & Appl Chem **74**: 1871
[13] Chou I-M, Sterner SM, Pitzer KS (1992) Geochim Cosmochim Acta **56**: 2281
[14] Fournier RO, Thompson JM (1993) Geochim Cosmochim Acta **57**: 4365
[15] Ravich MI, Borovaya FE (1950) Izv Sektora Fiz-Khim Analyza **20**: 165
[16] Sterner SM, Hall DL, Bodnar RJ (1988) Geochim Cosmochim Acta **52**: 989
[17] Ravich MI, Borovaya FE (1949) Izv Sektora Fiz-Khim Analyza **19**: 69
[18] Dingemans P (1939) Rec Trav Chim **58**: 559
[19] Dingemans P (1945) Rec Trav Chim **64**: 194
[20] Ravich MI, Borovaya FE, Luk'yanova EI, Elenevskaya VM (1954) Izv Sekt Fiz-Khim Analyza **24**: 280
[21] Itkina LS (1973) Lithium, Rubidium and Cesium Hydroxides (Russ). Nauka, Moscow
[22] Urusova MA, Valyashko VM (1998) Russ J Inorg Chem **43**: 948
[23] Valyashko VM, Urusova MA (1996) Russ J Inorg Chem **41**: 1297
[24] Peters CJ, Gauter K (1999) Chem Rev **99**: 419
[25] Schroeder WC, Berk AA, Gabriel A et al (1935, 1936, 1937) J Amer Chem Soc **57**: 1539, **58**: 843, **59**: 1783
[26] Valyashko VM (1973) Zh Neorgan Khimii **28**: 1114
[27] Ravich MI, Urusova MA (1967) Zh Neorgan Khimii **12**: 1335
[28] Valyashko VM (1990) Pure & Appl Chem **62**: 2129

[29] Valyashko VM (2000) In: Tremaine PR, Hill PG, Irish, DE, Balakrishnan PV (eds) Steam, Water and Hydrothermal Systems, Proc of the 13th Intern Conf on the Properties of Water and Steam. NRS Research Press, Ottawa, p 727
[30] Wetton EAM (1981) Power Ind Res **1**: 151
[31] Urusova MA, Valyashko VM (2001) Russ J Inorg Chem **46**: 777
[32] Valyashko VM, Ravich MI (1968) Zh Neorgan Khimii **13**: 1426
[33] Ravich MI, Borovaya FE (1968) Zh Neorgan Khimii **13**: 1418
[34] Ravich MI; Borovaya FE, Smirnova EG (1968) Zh Neorgan Khim **13**: 1922
[35] Boettcher AL, Wyllie PJ (1969) Geochim Cosmochim Acta **33**: 611
[36] Kennedy G, Wasserburg G, Heard M (1962) Amer J Sci **260**: 500
[37] Stewart DB (1967) Schweiz Miner Petrogr Mitt **47**: 35
[38] Valyashko VM, Kravchuk KG (1978) Dokl Akad Nauk SSSR **242**: 1104
[39] Ravich MI, Valyashko VM (1969) Zh Neorgan Khimii **14**: 1650